

UCSF

UC San Francisco Previously Published Works

Title

Endostatin Is a Trans-Synaptic Signal for Homeostatic Synaptic Plasticity

Permalink

<https://escholarship.org/uc/item/7dz8s179>

Journal

Neuron, 83(3)

ISSN

0896-6273

Authors

Wang, Tingting
Hauswirth, Anna G
Tong, Amy
[et al.](#)

Publication Date

2014-08-01

DOI

10.1016/j.neuron.2014.07.003

Peer reviewed

Published in final edited form as:

Neuron. 2014 August 6; 83(3): 616–629. doi:10.1016/j.neuron.2014.07.003.

Endostatin is a Trans-Synaptic Signal for Homeostatic Synaptic Plasticity

Tingting Wang, Anna G. Hauswirth, Amy Tong, Dion Dickman, and Graeme W. Davis*

Department of Biochemistry and Biophysics, University of California San Francisco, San Francisco, CA 94158, USA

Abstract

At synapses in organisms ranging from fly to human, a decrease in postsynaptic neurotransmitter receptor function elicits a homeostatic increase in presynaptic release that restores baseline synaptic efficacy. This process, termed presynaptic homeostasis, requires a retrograde, trans-synaptic signal of unknown identity. In a forward genetic screen for homeostatic plasticity genes we identified *multiplexin*. Multiplexin is the *Drosophila* homologue of Collagen XV/XVIII, a matrix protein that can be proteolytically cleaved to release Endostatin, an anti-angiogenesis signaling factor. Here we demonstrate that Multiplexin is required for normal calcium channel abundance, presynaptic calcium influx and neurotransmitter release. Remarkably, Endostatin has a specific activity, independent of baseline synapse development that is required for the homeostatic modulation of presynaptic calcium influx and neurotransmitter release. Our data support a model in which proteolytic release of Endostatin signals trans-synaptically, acting in concert with the presynaptic CaV2.1 calcium channel, to promote presynaptic homeostasis.

Keywords

Multiplexin; Endostatin; Extracellular matrix; Synaptic homeostasis; Calcium channel; CaV2.1; Retrograde signaling; Homeostatic plasticity; Synaptic homeostasis; Neuromuscular junction; Epilepsy; Schizophrenia; Autism; Synaptic transmission; Neuron

Introduction

The nervous system is continually modified by experience. Given the tremendous complexity of the nervous system, it is astounding that robust and reproducible neural function can be sustained throughout life. It is now apparent that homeostatic signaling systems stabilize the excitable properties of nerve and muscle and, thereby, constrain how the nervous system can be altered by experience or crippled by disease. The *Drosophila*

© 2014 Elsevier Inc. All rights reserved.

*Correspondence: graeme.davis@ucsf.edu.

Supplemental Information: Supplemental information includes methods, four figures and one table.

Publisher's Disclaimer: This is a PDF file of an unedited manuscript that has been accepted for publication. As a service to our customers we are providing this early version of the manuscript. The manuscript will undergo copyediting, typesetting, and review of the resulting proof before it is published in its final citable form. Please note that during the production process errors may be discovered which could affect the content, and all legal disclaimers that apply to the journal pertain.

neuromuscular junction (NMJ) has emerged as a powerful model system to dissect the underlying mechanisms that achieve the homeostatic modulation of presynaptic neurotransmitter release. At the *Drosophila* NMJ, inhibition of postsynaptic glutamate receptor function causes a homeostatic increase in presynaptic neurotransmitter release that precisely restores muscle excitation to baseline levels. This phenomenon is conserved from fly to human (Cull-Candy et al., 1980; Plomp et al., 1992). Importantly, presynaptic homeostasis has also been observed at mammalian central synapses *in vitro* in response to differences in target innervation (Liu and Tsien, 1995), altered postsynaptic excitability (Burrone et al., 2002) and following chronic inhibition of neural activity (Kim and Ryan, 2010; Zhao et al., 2011).

Despite progress in identifying presynaptic effector proteins that are required for the expression of presynaptic homeostasis (Davis, 2013), the identity of the retrograde signaling system remains unknown. Numerous neurotrophic factors, such as nerve growth factor (NGF), brain derived neurotrophic factor (BDNF), glia-derived neurotrophic factor (GDNF), as well as nitric oxide, endocannabinoids and adhesion molecules are identified as retrograde signals that regulate presynaptic cell survival, differentiation and biophysical properties in an activity-dependent manner (Gottmann, 2008; Harrington and Ginty, 2013; Iremonger et al., 2013). Among these molecules, BDNF has been implicated in the trans-synaptic control of presynaptic release in cultured hippocampal neurons (Jakawich et al., 2010). It was previously demonstrated that a bone morphogenetic protein (BMP) ligand (glass bottom boat) is released from muscle, activates a type II BMP receptor at the presynaptic terminal and is required for the growth of the presynaptic nerve terminal (McCabe et al., 2003). This BMP signaling system is also necessary for presynaptic homeostasis. However, the BMP signaling system is a permissive signal that acts at the motoneuron cell body (Goold and Davis, 2007).

A large-scale, electrophysiology-based forward genetic screen for mutations that block presynaptic homeostasis (Dickman and Davis, 2009; Muller et al., 2011) identified *multiplexin* as a candidate homeostatic plasticity gene. *Drosophila* Multiplexin is the homologue of human Collagen XV and XVIII, matrix molecules that are expressed ubiquitously in various vascular and epithelial basement membranes throughout the body (Seppinen and Pihlajaniemi, 2011). Mutations in the human *COL18A1* gene cause Knobloch syndrome, characterized by retinal detachment, macular abnormalities and occipital encephalocele (Passos-Bueno et al., 2006; Sertie et al., 2000; Suzuki et al., 2002). Patients with Knobloch syndrome are also predisposed to epilepsy (Suzuki et al., 2002), highlighting the critical function of Collagen XVIII in the central nervous system. Moreover, the C-terminal of Collagen XVIII, encoding an Endostatin domain, can be cleaved proteolytically (Chang et al., 2005; Felbor et al., 2000; Heljasvaara et al., 2005), and functions as an anti-angiogenesis factor to inhibit tumor progression (Dhanabal et al., 1999; O'Reilly et al., 1997; Yamaguchi et al., 1999). Endostatin inhibits angiogenesis by interacting with various downstream signaling factors, including vascular endothelial growth factor receptors (VEGFR) (Kim et al., 2002), integrins (Wickstrom et al., 2002), and Wnt signaling molecules (Hanai et al., 2002). Little is known regarding the function of *multiplexin* in the nervous system. Here, we provide evidence that Endostatin, a proteolytic cleavage product

of *Drosophila* Multiplexin, functions as a trans-synaptic signaling molecule that is essential for the homeostatic modulation of presynaptic neurotransmitter release at the *Drosophila* NMJ.

Results

Multiplexin Required for the Rapid Induction of Synaptic Homeostasis

Application of philanthotoxin (PhTX) to the *Drosophila* NMJ, at sub-blocking concentrations, inhibits postsynaptic glutamate receptor function and leads to a homeostatic potentiation of presynaptic neurotransmitter release, termed presynaptic homeostasis (Frank et al., 2006). This assay is the basis for an ongoing, electrophysiology-based forward genetic screen for mutations that block presynaptic homeostasis (Dickman and Davis, 2009; Muller et al., 2011). This screen identified a transposon insertion ($pBac^{f07253}$) in the *Drosophila multiplexin* gene that blocks PhTX induced presynaptic homeostasis (Figure 1A). The expression of the *multiplexin* gene is complex with multiple splice variants and three major protein isoforms (Figure 1B; (Meyer and Moussian, 2009); www.flybase.org). The $pBac^{f07253}$ transposon insertion resides within an intron and has been reported to disrupt expression of the long and middle isoforms of Multiplexin, indicating it is a loss-of-function allele (Momota et al., 2011).

First, we confirmed that loss of *multiplexin* disrupts the rapid induction of synaptic homeostasis. Bath application of 20 μ M PhTX induced a significant decrease in mEPSP amplitude at both wild-type and dmp^{f07253} mutant synapses (Figure 1C and 1D). At wild-type synapses, an increase in presynaptic release (Figure 1C and 1D; quantal content) was observed to offset the change in mEPSP amplitude and restore postsynaptic excitation to baseline values (Figure 1C). By contrast, following application of PhTX to the dmp^{f07253} mutant there was no change in quantal content and EPSPs were significantly smaller than that observed in the dmp^{f07253} mutant in the absence of PhTX (Figure 1C and 1D). Presynaptic homeostasis was also blocked when dmp^{f07253} was placed *in trans* to a deficiency [$Df(3L)BSC224$] that uncovers the entire *multiplexin* locus (Figure 1D). Thus, loss of function mutations in *multiplexin* block presynaptic homeostasis. Throughout this paper, average values are presented in figures with sample sizes reported in figure legends. Absolute values of mEPSP amplitudes, EPSP amplitudes and quantal contents for each data set are included in Table S1.

In these initial experiments, we discovered that baseline EPSP amplitudes and quantal contents recorded in dmp^{f07253} and dmp^{f07253}/df mutant synapses were significantly decreased compared to wild-type and heterozygous controls (Figure 1G and 1H; $p < 0.001$). Since there was no change in average mEPSP amplitude, the data imply a defect in baseline presynaptic release (Figure 1F). However, analysis of a second transposon insertion mutation, dmp^{c01251} , demonstrates that synaptic homeostasis is blocked without a concomitant change in baseline release (Figure 1A; www.flybase.org). At dmp^{c01251} mutant synapses, there was a minor deficit in baseline spontaneous mEPSP amplitude (Figure 1F; $p < 0.005$) and quantal content (Figure 1H; $p < 0.005$), but the average EPSP amplitude is similar to wild-type (Figure 1G; N.S., $p = 0.24$). When PhTX was applied to the dmp^{c01251} synapses, homeostasis was blocked. Specifically, the average mEPSP amplitude at

dmp^{C01251} synapses was decreased by ~50%, but quantal content was unaltered (Figure 1C and 1D). Finally, to address whether the efficient induction of presynaptic homeostasis is sensitive to the extracellular concentration of calcium, we assayed presynaptic homeostasis at *dmp*^{f07253} mutant synapses at an elevated extracellular calcium concentration (1mM). Raising extracellular calcium increases the average EPSP amplitude from ~ 15 mV to ~ 30mV at *dmp*^{f07253} synapses, a value similar to wild-type at 0.4mM extracellular calcium, but presynaptic homeostasis remained blocked (Figure 1E). Taken together, these data demonstrate that Multiplexin is necessary for presynaptic homeostasis and has a separable, required function to promote baseline presynaptic neurotransmitter release (see below for additional evidence).

Endostatin is Sufficient to Rescue Synaptic Homeostasis in *multiplexin* Mutants

Multiplexin is the *Drosophila* homologue of human Collagen XV/XVIII. In mammals, Collagen XVIII is proteolytically cleaved to release a C-terminal domain termed “Endostatin” which has been shown to have anti-angiogenic activity (Figure 2A;(Myllyharju and Kivirikko, 2004; O'Reilly et al., 1997)). *Drosophila* Multiplexin also contains a C-terminal Endostatin domain and is expressed in both neurons and muscles (Momota et al., 2011). In order to test whether *Drosophila* Endostatin might participate in presynaptic homeostasis we attempted to rescue *multiplexin* mutants by over expressing a *UAS-endostatin* transgene either pre- or postsynaptically.

First, we demonstrate that Endostatin is trafficked to the NMJ (Figure 2B and 2C). We generated and expressed a *UAS-endostatin-GFP* transgene in wild-type animals using pan-neuronal (*elav*^{C155}-*Gal4*) or muscle-specific drivers (*MHC-Gal4*). Structured Illumination Microscopy (SIM) images were acquired from synapses co-labeled for the active zone marker Bruchpilot (Brp) and Endostatin-GFP (ES-GFP; Figure 2B, 2C and S1A). We find that presynaptically expressed Endostatin-GFP forms punctate structures that are distributed throughout the presynaptic nerve terminal (Figure 2B). In some cases, Endostatin-GFP is localized in the center of ring-shaped active zones (Figure 2C, right upper panels) facing the extracellular space (Figure 2C, right lower panels), indicating that Endostatin-GFP is trafficked to synapses. When expressed by a muscle-specific driver (*MHC-Gal4*), Endostatin-GFP is found across the entire muscle, without enrichment at the postsynaptic NMJ (Figure S1A). In order to determine whether Endostatin-GFP is expressed and secreted to the extracellular matrix, we performed immunolabeling to examine the surface expression of Endostatin-GFP achieved by staining without permeabilizing the cell (Figure S1B-S1D). We find that Endostatin-GFP is expressed and forms punctate structures on the cell surface when expressed pre- (Figure S1B, *elav*^{C155}-*Gal4*>*UAS-endostatin-GFP*) or postsynaptically (Figure S1C, *BG57-Gal4*>*UAS-endostatin-GFP*). As a control, we showed that a GFP-tagged cytoplasmic protein is not detectable in the absence of cell permeabilization (Figure S1D, *elav*^{C155}-*Gal4*>*UAS-s6k-GFP*).

Next, we examined whether overexpression of Endostatin can functionally restore baseline transmission and synaptic homeostasis in *multiplexin* mutants. We expressed Endostatin (*UAS-endostatin*; (Meyer and Moussian, 2009)) in neurons and muscles of *dmp*^{f07253} mutant animals, using either pan-neuronal (*elav*^{C155}-*Gal4*) or muscle specific (*MHC-Gal4*) drivers

(Figure 2D-2H). First, we find that both neuron-specific and muscle-specific expression of Endostatin rescues baseline neurotransmission at the *dmp^{f07253}* mutant NMJ (Figure 2D and 2F-2H). Second, we find that both neuron-specific and muscle-specific expression of Endostatin rescues PhTX-induced synaptic homeostasis at the *dmp^{f07253}* mutant NMJ (Figure 2D and 2E). Additional controls were performed to confirm that the rescue of synaptic homeostasis is caused by the overexpression of Endostatin and is not an effect that could have been contributed by the insertion sites of either the *Gal4* drivers or the *UAS* transgene (Figure S2). PhTX induced synaptic homeostasis was completely blocked in *dmp^{f07253}* mutants harboring the *UAS-endostatin* transgene without a source of Gal4 (Figure S2A and S2B), and was also blocked in *dmp^{f07253}* mutants harboring a pan-neuronal (Figure S2B, *elav^{C155}-Gal4;;dmp^{f07253}*) or muscle-specific Gal4 driver without *UAS-endostatin* (Figure S2B, *MHC-Gal4,dmp^{f07253}*). Similar controls were also performed for analysis of baseline neurotransmission (Figure S2C-S2E). Finally, we expressed an untagged Endostatin transgene (*UAS-endostatin*) in neurons, muscles or both neurons and muscles of wild-type animals, using either pan-neuronal (*elav^{C155}-Gal4*) or muscle-specific (*MHC-Gal4*) or both drivers (*OK371-Gal4;BG57-Gal4*, Figure S3). We find that all genotypes showed normal basal synaptic transmission compared to wild-type synapses, indicating that Endostatin has an activity that requires the context of homeostatic plasticity, perhaps acting in concert with the protease responsible for Endostatin release or with presynaptic ENaC channels implicated in presynaptic homeostasis (see discussion; Younger et al., 2013). Taken together, these data are consistent with Endostatin acting as a trans-synaptic signaling molecule that is required for presynaptic homeostasis.

Synaptic Morphology is Normal in *multiplexin* Mutants

It has been demonstrated that *Drosophila multiplexin* is involved in motor axon path finding at the NMJ and regulates wingless distribution in the embryo (Meyer and Moussian, 2009; Momota et al., 2011). Multiplexin homologues in other systems have been shown to participate in anatomical neural development (Ackley et al., 2001; Ackley et al., 2003). Therefore, we examined pre- and postsynaptic morphology at the NMJ of muscle 4 in abdominal segment 2 and 3 by immuno-labeling the presynaptic active zone component Bruchpilot (Brp, Figure 3A) and the postsynaptic protein Discs-large (Dlg, Figure 3A). We find that total active zone numbers, estimated by quantification of Brp puncta, are similar when comparing wild-type to the *dmp^{f07253}* mutant, as well as to two additional domain specific mutant alleles, *dmp^N* and *dmp^C*, which remove the N- and C-terminal portions of Multiplexin (Figure 1A, 1B and 3B). We next probed the absolute number of boutons per NMJ on muscle 6/7 at abdominal segment 2 and 3. The total bouton numbers at *dmp^{f07253}* and *dmp^N* NMJs were not significantly different than wild-type (Figure 3C), whereas the *dmp^C* mutant had slightly elevated bouton numbers compared to wild-type, but only on abdominal segment 2 (Figure 3C; $p < 0.001$). In conclusion, the disruption of homeostasis and the change in baseline transmission observed in *multiplexin* mutants cannot be attributed to impaired anatomical development or decreased active zone numbers at the NMJ.

Multiplexin is Required for Presynaptic Calcium Channel Localization

The observed defect in baseline transmission without a change in active zone number suggests a change in presynaptic release probability. To explore the underlying cause, we

examined the abundance and distribution of presynaptic calcium channels at the *dmp*^{f07253} mutant NMJ. To do so, we over-expressed a GFP-tagged CaV2.1 calcium channel α subunit, (*UAS-cac-GFP*; (Kawasaki et al., 2004)) using the pan-neuronal driver *elav*^{C155}-*Gal4* in either wild-type or the *dmp*^{f07253} mutant background (Figure 4). Presynaptic active zones were simultaneously visualized by immunolabeling for Bruchpilot (Brp, Figure 4A-4D). Confocal images were collected at muscle 6/7 in abdominal segment 2 and 3 (Figure 4A and 4B). Synaptic Cac-GFP fluorescence intensities, defined as the average Cac-GFP intensity inside each Brp punctum (see Experimental Procedures for detail), were quantified at *dmp*^{f07253} and wild-type NMJ. The *dmp*^{f07253} mutants showed a 23% decrease in synaptic Cac-GFP intensity (Figure 4E and 4F; $p < 0.0001$), indicating that CaV2.1 calcium channels are less abundant at the NMJ in the *dmp*^{f07253} mutants. To confirm this effect, we acquired Cac-GFP images with Structured Illumination Microscopy (SIM) and quantified synaptic Cac-GFP volumes based on reserved raw fluorescence intensity values (see Experimental Procedures for detail). Fluorescent SIM images of Cac-GFP and Brp were collected on muscle 6/7 in abdominal segment 2 and 3 in *dmp*^{f07253} and wild-type (Figure 4C and 4D). As described previously (Liu et al., 2011), presynaptic active zones form ring-shaped structures with CaV2.1 calcium channels localized in the center (Figure 4C). Ring-shaped active zones with calcium channels were observed in both *dmp*^{f07253} and wild-type synapses, suggesting that active zone organization is normal in *dmp*^{f07253} mutants. In order to quantify the abundance of synaptic CaV2.1 calcium channels at presynaptic active zones, we computationally associated each Cac-GFP volume with a Brp ring in close proximity (see Experimental Procedures for detail). Only Cac-GFP puncta paired with nearby Brp-positive active zones were defined as synaptic calcium channels and were used for quantification. Fluorescence intensity values, non-normalized during image processing, were used to estimate Cac-GFP volume (see methods). The average Cac-GFP volume at *dmp*^{f07253} synapses decreased 19% compared to wild-type (Figure 4G and 4H; $p < 0.0001$), supporting the conclusion that presynaptic CaV2.1 channels are less abundant in *dmp*^{f07253} mutants. From these data, we conclude Multiplexin is necessary for the normal abundance of presynaptic, active zone localized, CaV2.1 calcium channels.

Multiplexin Mutants Exhibit Defects in Short-Term Plasticity and Presynaptic Calcium Influx

We next sought to determine whether fewer synaptic calcium channels at *dmp*^{f07253} mutant synapses alter synaptic function. If there are fewer calcium channels per active zone, then we expect to observe a decrease in presynaptic calcium influx and a decrease in presynaptic release probability. We confirmed both predictions. To assess a change in presynaptic release probability, we examined short-term facilitation and depression during stimulus trains. At *dmp*^{f07253} mutant synapses, we observed significant facilitation during a 20Hz stimulus train, whereas there was pronounced synaptic depression at wild-type synapses (Figure 5A and 5B). It should be noted that the steady state EPSP amplitude in *dmp*^{f07253} mutants during a 20Hz train plateaus and never reaches wild-type levels (Figure 5B). This indicates that the defect in presynaptic release probability cannot be restored during a stimulus train by an increase of intracellular calcium that occurs during a train. Consistent with this finding, the *dmp*^{f07253} mutant synapses also show a decrease in presynaptic release over a range of extracellular calcium concentrations (0.2-0.5mM), while the apparent

cooperativity of release remains similar to wild type (Figure 5C). When we examined synaptic facilitation at low extracellular calcium (0.2mM), we again observed that *dmp*^{f07253} mutant synapses showed facilitation compared to wild-type synapses that depressed over a range of inter-stimulus intervals (Figure 5D). The steady state EPSP amplitude in *dmp*^{f07253} mutants was also significantly smaller than that in wild-type animals during 20Hz and 10Hz trains at low extracellular calcium (Figure 5E and 5F). Taken together, these data support the conclusion that there is a drop in presynaptic release probability at *dmp*^{f07253} mutant synapses compared to wild-type.

Next, we examined presynaptic calcium influx by imaging the spatially averaged presynaptic calcium signal at wild-type and *dmp*^{f07253} mutant boutons following single action potential stimulation. The spatially averaged calcium transients were attained by loading presynaptic terminals with the calcium indicator Oregon green 488 BAPTA-1 (OGB-1) and a reference dye, Alexa 568. Single AP-evoked calcium transients were quantified using line scans across type 1b boutons on muscle 6/7 in abdominal segments 2 and 3 (see Experimental Procedures for detail). As exemplified in Figure 5G, we found that the average peak amplitude of single AP-evoked calcium transients in the *dmp*^{f07253} mutant was significantly smaller than observed at wild-type synapses (Figure 5H and 5I; $p < 0.001$). As a control, baseline OGB-1 fluorescence before stimulus onset was not different between genotypes (Figure 5J, $p=0.11$), indicating similar OGB-1 loading in *dmp*^{f07253} mutant and wild-type synapses. Taken together, our data provide evidence that loss of the *multiplexin* gene causes a decrease in presynaptic calcium channel abundance with a corresponding drop in both presynaptic calcium influx and presynaptic release probability. We conclude that Multiplexin is necessary for establishing or maintaining wild-type calcium channel abundance at the presynaptic active zone.

The N- and C-terminal Domains of Multiplexin Have Discrete Functions Controlling Baseline Transmission and Presynaptic Homeostasis

Different structural domains have been identified in Multiplexin, including a Thrombospondin-like domain, collagen triple helix, trimerization region, hinge region and C-terminal Endostatin domain (Meyer and Moussian, 2009). In order to dissect the contribution of these domains to baseline release and presynaptic homeostasis, we examined the induction of synaptic homeostasis in two deletion mutants, one that removes the N-terminal Thrombospondin-like domain and a second that removes the C-terminal Endostatin domain (Figure 6A). Intriguingly, the N- and C-terminal domains confer different activities (Figure 6). The N-terminal deletion mutant (*dmp*^N) exhibits a significant decrease in average baseline EPSP amplitude and quantal content (Figure 6B, 6E and 6F; $p < 0.001$), but showed only minor suppression of presynaptic homeostasis (Figure 6B and 6C). By contrast, the C-terminal deletion mutant (*dmp*^C) has little or no effect on baseline EPSP and quantal content (Figure 6E, $p=0.08$; Figure 6F, $p < 0.05$), but completely blocks presynaptic homeostasis (Figure 6B and 6C). These data suggest that the N-terminal Thrombospondin-like domain is required for basal transmission, while the C-terminal Endostatin domain is required for presynaptic homeostasis. By extension, the phenotype observed in the *dmp*^C mutant clearly dissociates the function of Endostatin during presynaptic homeostasis and baseline transmission.

As a control, we examined short-term plasticity in the *dmp^C* mutant. If the *dmp^C* mutant NMJ has wild-type baseline transmission, then short-term synaptic plasticity should also be similar to wild-type. We examined baseline synaptic transmission during a 20Hz stimulus train and at different extracellular calcium concentrations. Similar to wild-type, *dmp^C* mutant synapses showed synaptic depression and wild-type steady state EPSP amplitudes during a 20Hz train (Figure 6G and 6H). Furthermore, the apparent calcium cooperativity of neurotransmitter release in *dmp^C* mutant was not different compared to wild-type synapses (Figure 6I). Finally, *dmp^C* mutant synapses had normal paired-pulse ratios and short-term synaptic plasticity at low extracellular calcium concentration compared to wild-type synapses (Figure 6J-6L). Thus, the Endostatin domain has a highly specific, required function for the homeostatic modulation of neurotransmitter release.

Finally, we explored the underlying mechanism that may cause the discrete effect on basal synaptic transmission in the *dmp^N* and *dmp^C* mutants. We examined the abundance of presynaptic calcium channels at the *dmp^N* and *dmp^C* mutant NMJ. We over-expressed a GFP-tagged CaV2.1 calcium channel α subunit, (*UAS-cac-GFP*) using the pan-neuronal driver *elav^{C155}-Gal4* in either wild-type or the *dmp^N* or *dmp^C* mutant backgrounds (Figure S4). Presynaptic active zones were simultaneously visualized by immunolabeling for Bruchpilot at muscle 6/7 in abdominal segment 2 and 3. We find that there is a 15% reduction of synaptic Cac-GFP intensity at *dmp^N* mutant synapses (Figure S4A, S4B and S4D-S4E; $p < 0.0001$), indicating that CaV2.1 calcium channels are less abundant at the NMJ in the *dmp^N* mutant. Importantly, *dmp^C* mutant synapses showed completely normal presynaptic Cac-GFP intensity at active zones (Figure S4A, S4C-S4E; $p=0.5849$), consistent with our hypothesis that N-terminal thrombospondin-like domain but not C-terminal Endostatin domain is required for maintaining normal presynaptic calcium channel abundance and synaptic transmission at basal condition.

Endostatin Regulates the Sustained Expression of Presynaptic Homeostasis

A homeostatic increase in presynaptic release can be persistently induced by genetic deletion of the postsynaptic ionotropic glutamate receptor subunit GluRIIA (Petersen et al., 1997). To test whether *multiplexin* is required for the maintenance of synaptic homeostasis, we generated double mutant flies harboring mutations in *GluRIIA* and *multiplexin*. The *GluRIIA^{sp16}* mutation alone caused a significant reduction of mEPSP amplitude that was offset by a homeostatic increase of presynaptic release, which restored EPSP amplitudes to wild-type values (Figure 7A and 7B; (Petersen et al., 1997)). We then examined three different *GluRIIA* and *multiplexin* double mutant combinations: *GluRIIA^{sp16};dmp^{f07253}*, as well as *GluRIIA^{sp16};dmp^N* and *GluRIIA^{sp16};dmp^C*. In all of the double mutants, the mEPSP amplitudes are significantly decreased compared to *dmp^{f07253}*, *dmp^N* and *dmp^C* mutants alone (Figure 7A and 7B). Interestingly, homeostatic modulation of presynaptic release was normal in *GluRIIA^{sp16};dmp^{f07253}* and *GluRIIA^{sp16};dmp^N* double mutants, but was blocked in *GluRIIA^{sp16};dmp^C* mutant (Figure 7A and 7B). Thus, the sustained expression of homeostatic plasticity induced by the *GluRIIA^{sp16}* mutation is only disrupted in the *dmp^C* mutant. An explanation for this finding is based on a previous study that demonstrated by PCR that Endostatin mRNA is completely lost in the *dmp^C* mutant, whereas a small amount of Endostatin persists in the *dmp^{f07253}* mutant (Momota et al.,

2011). We conclude that both the rapid induction and long-term maintenance of synaptic homeostasis require Endostatin, but with different sensitivities. Decreased levels of Endostatin prevents the rapid induction of presynaptic homeostasis. However, if the disruption of GluRIIA persists, then small amounts of Endostatin are sufficient to mediate long-term presynaptic homeostasis.

Endostatin is Necessary for the Homeostatic Modulation of Presynaptic Calcium Influx

Mutations in *multiplexin* cause defects in synaptic transmission, release probability, and decreases in presynaptic calcium channel abundance and presynaptic calcium influx. Therefore, we pursued experiments to test the possibility that Multiplexin functions in concert with CaV2.1 calcium channels during the rapid induction of synaptic homeostasis. First, we sought to determine whether *multiplexin* genetically interacts with the CaV2.1 calcium channel α subunit, which was previously shown to be required for synaptic homeostasis (Frank et al., 2006). A CaV2.1 α -subunit mutation, *cac^s*, when tested as a heterozygous mutation *in trans* to a wild-type chromosome, had no effect on synaptic homeostasis (Figure 8B). Similarly, a heterozygous mutation of *dmp^{f07253}* does not alter synaptic homeostasis (Figure 8B). However, homeostatic compensation was completely blocked when the *cac^s* mutation was placed *in trans* to the *dmp^{f07253}* mutation in a double-heterozygous condition (Figure 8A and 8B). Genetic interaction experiments were then conducted with the *dmp^C* mutant with similar results (Figure 8A and 8C).

Both the rapid induction and sustained expression of synaptic homeostasis are correlated with a statistically significant increase in presynaptic calcium influx (Muller and Davis, 2012). Furthermore, *multiplexin* is necessary for normal baseline calcium channel abundance and calcium influx. Therefore, we tested whether Endostatin might function as a trans-synaptic signal that controls the homeostatic modulation of presynaptic calcium influx. As previously reported, average peak amplitude for single AP-evoked calcium transients was significantly larger in *GluRIIA^{sp16}* mutant than in wild-type synapses (Figure 8D and 8E; $p < 0.0001$). Although we observed a slight decrease of baseline fluorescence, this is unlikely to account for the full effect of increase of presynaptic calcium influx in the *GluRIIA^{sp16}* mutant based on previous publications (Figure 8F; $p=0.051$; Muller et al., 2011; Muller and Davis, 2012). Next, we examined presynaptic calcium influx in the *dmp^C* mutant and the *GluRIIA^{sp16};dmp^C* double mutant synapses. Interestingly, there was no significant difference of calcium transient peak amplitudes between the *dmp^C* mutant and *GluRIIA^{sp16};dmp^C* double mutants (Figure 8D and 8E; $p=0.985$). As a control, there was no significant change in baseline fluorescence between *dmp^C* mutant and *GluRIIA^{sp16};dmp^C* double mutant (Figure 8G; $p=0.536$). Thus, the homeostatic modulation of presynaptic calcium influx is blocked in *GluRIIA^{sp16};dmp^C* double mutants. Consistent with our observation of normal synaptic transmission and presynaptic calcium channel abundance, the *dmp^C* mutant has normal presynaptic calcium influx compared to wild-type synapses (Figure 8D and 8E; $p=0.747$). Our data indicate that Endostatin is a trans-synaptic signal that is required for an increase in presynaptic calcium influx during presynaptic homeostasis. Based on these genetic interaction data and the finding that Endostatin is necessary for the modulation of presynaptic calcium influx during homeostatic plasticity, we

conclude that Multiplexin functions in concert with the CaV2.1 calcium channels to control the homeostatic modulation of neurotransmitter release.

Discussion

Here we provide evidence that Endostatin is a trans-synaptic signal for the homeostatic modulation of presynaptic neurotransmitter release. Specifically, we show that loss of Endostatin blocks the homeostatic modulation of presynaptic calcium influx and presynaptic neurotransmitter release. This activity is remarkably specific to presynaptic homeostasis, since loss of Endostatin has no effect on baseline neurotransmission or synapse morphology. Endostatin also interacts genetically with the pore-forming subunit of the CaV2.1 calcium channel and is required for the homeostatic increase of presynaptic calcium influx during synaptic homeostatic plasticity. Finally, transgenic overexpression of Endostatin is sufficient to rescue synaptic homeostasis and baseline neurotransmitter release when it is supplied to either the pre- or postsynaptic side of the synapse. Although deletion of Endostatin does not impair baseline transmission, overexpression of Endostatin in the *dmp*^{f07253} mutant is sufficient to restore baseline transmission release even in the absence of the Thrombospondin-like domain. As a working model, we propose that inhibition of postsynaptic glutamate receptors initiates the proteolytic cleavage of Multiplexin, which resides in the synaptic cleft. We further propose that release of Endostatin acts upon presynaptic calcium channels, directly or indirectly, to potentiate calcium influx and presynaptic neurotransmitter release (Figure 8G). This model is consistent with data from other systems demonstrating that activation of Endostatin requires proteolytic cleavage of Collagen XVIII by matrix metalloproteases (MMP) and cysteine cathepsins. Moreover, only free Endostatin released by cleavage functions as an anti-angiogenesis factor (Heljasvaara et al., 2005).

Endostatin Regulates Homeostatic Plasticity

The means by which presynaptic calcium channel function is modulated by Endostatin (Figures 4, 5) remains to be elucidated. Recently, it has been shown that a presynaptic Deg/ENaC channel is also necessary for the homeostatic modulation of presynaptic release (Younger et al., 2013). In this previous study, a model is presented in which ENaC channel insertion causes a sodium leak and modest depolarization of the presynaptic resting membrane potential that, in turn, potentiates presynaptic calcium influx. One possibility is that the interaction of Endostatin with the presynaptic CaV2.1 channels enables the channels to respond to low-voltage modulation. This would be consistent with both Endostatin and the ENaC channel being strictly necessary for presynaptic homeostasis. It remains formally possible that Endostatin stabilizes presynaptic ENaC channels and, thereby, influences presynaptic calcium influx. For example, it was demonstrated that the interaction between ENaC channels and extracellular collagens mediates the mechanosensory transduction in the touch reception systems (Chalfie, 2009; Liu et al., 1996).

Proteolytic Cleavage of Synaptic Proteins as a Trigger for Retrograde Trans-Synaptic Signaling

Activation of Endostatin in other systems requires proteolytic cleavage of Collagen XVIII by matrix metalloproteases (MMP) and cysteine cathepsins. This raises an intriguing possibility that, during synaptic homeostasis, Multiplexin could be cleaved by synaptic MMPs, releasing Endostatin to trigger a homeostatic change in presynaptic release. In this model, inhibition of postsynaptic glutamate receptors would lead to the activation of MMPs within the synaptic cleft (Figure 8G). Thus, the retrograde signal would be a multi-stage system, providing opportunity for both amplification and multi-level control of the signaling event. At glutamatergic synapses in hippocampal neurons, proteolytic cleavage of neuroligin-1, a synaptic adhesion molecule residing in postsynaptic terminals, is triggered by postsynaptic NMDA receptor activation. Cleavage of neuroligin-1 depresses presynaptic transmission by reducing presynaptic release probability in a trans-synaptic manner (Peixoto et al., 2012). Thus, the activity-dependent cleavage of cell adhesion and extracellular matrix proteins could provide a robust and evolutionarily conserved feedback paradigm for trans-synaptic signaling to regulate synaptic efficacy in diverse neuronal circuits.

Experimental Procedures

Fly Stocks and Genetics

All fly stocks were maintained at 22-25°C on normal food. All flies were obtained from Bloomington *Drosophila* Stock Center or the Exelixis Collection (Harvard Medical School), unless otherwise noted. The *multiplexin* N- (*dmp^N*) and C-terminal (*dmp^C*) deletion mutations and Endostatin rescue allele (*UAS-endostatin*) were generous gifts from Bernard Moussian (Max-Planck-Institute for Developmental Biology, Tübingen, Germany). For pan-neuronal expression, we used driver *elav^{C155}-Gal4* on the X chromosome (male larvae), for muscle expression, we used *MHC-Gal4* or *BG57-Gal4* (as specified in Figure Legends or Results), for neuronal and muscle expression, we used *OK371-Gal4;BG57-Gal4*. Unless otherwise noted, the *w¹¹¹⁸* strain was used as a wild-type (wt) control.

Electrophysiology

Electrophysiology was performed as described previously (Muller et al., 2011) using modified HL3 saline at the specified calcium concentrations containing the following components: NaCl (70mM), KCl (5mM), MgCl₂ (10mM), NaHCO₃ (10mM), Sucrose (115mM), Trehalose (5mM), HEPES (5mM), and CaCl₂ (0.4mM, unless specified otherwise). Mean EPSP, mEPSP amplitude and quantal content were obtained by averaging values across all NMJs for a given genotype. EPSP and mEPSP traces were analyzed in IGOR Pro (WaveMetrics) and MiniAnalysis (Synaptosoft).

Immunocytochemistry

Standard immunocytochemistry was performed as previously described. For surface GFP immuno-labeling, dissected third instar larvae were incubated with primary antibody for 20 min at room temperature and fixed with ice-cold ethanol. The following primary antibodies were used: mouse anti-Bruchpilot (Brp, 1:100) (Kittel et al., 2006), rabbit anti-Discs large

(Dlg, 1:1,000) (Pielage et al., 2008), rabbit anti-GFP (1:1,000, Invitrogen G10362), mouse anti-GFP (1:1,000, Invitrogen clone 3E6). Rabbit and mouse anti-GFP antibodies were used to detect surface and total GFP expression respectively. Alexa-conjugated secondary antibodies were used at 1:300 (Jackson Immuno-research Laboratories).

Image Acquisition and Analysis

Deconvolution imaging for synapse morphology was performed using a 100x (1.4 NA) plan Apochromat objective (Carl Zeiss) on an Axiovert 200 inverted microscope (Carl Zeiss) equipped with a cooled CCD camera (CoolSNAP HQ; Roper Scientific). Image acquisition and analysis were performed in SlideBook software (Intelligent Imaging Innovation). Maximum projections of deconvolved images were used for analyses. Quantification of Brp and bouton number was performed as previously described (Pielage et al., 2008). Confocal imaging was performed on a Yokogawa CSU22 spinning disk confocal with a 60x/1.4 plan Apochromat objective. Structured illumination fluorescence imaging for Endostatin-GFP and calcium channels was performed using an ELYRA PS.1 system (Carl Zeiss) with an inverted LSM 710 microscope equipped with a 63x(1.4 NA) plan Apochromat objective (Carl Zeiss) and an Andor iXon 885 EMCCD camera. For quantitative calcium channel abundance analysis, raw fluorescence intensities were preserved with position information using a customized algorithm (Carl Zeiss). See supplemental methods for details.

Calcium Imaging

Calcium imaging experiments at the third instar NMJ were performed as previously described (Muller and Davis, 2012) using 5 mM Oregon-Green 488 BAPTA-1 (OBG-1) (Invitrogen) and 1 mM Alexa 568 (Invitrogen). Image acquisition was performed at room temperature using a confocal laser-scanning system (Ultima, Prairie Technologies) equipped with excitation light (488 nm) from an air-cooled krypton-argon laser, 60x objective (1.0 NA, Olympus), and a gallium arsenide phosphide-based photocathode photomultiplier tube (Hamamatsu). Line scans across single boutons were made at a frequency of 568 Hz. Data of experimental and control groups were collected side by side. Calcium imaging data were acquired using Prairie View (Prairie Technologies) and analyzed in Igor Pro (Wavemetrics).

Supplementary Material

Refer to Web version on PubMed Central for supplementary material.

Acknowledgments

We thank Meg Younger, Mike Gavino, Kevin Ford and Cody Locke for critical reading of the manuscript. We thank Martin Müller for help with train stimulation data analysis in IGOR. We thank Bryant Chhun (Carl Zeiss) for help with custom algorithm to preserve raw fluorescence intensity in SIM images. We thank Tao Cui (California Institute of Technology) for help with SIM data processing by generating custom analysis program in Matlab. We thank Gama Ruiz for technical assistance. We thank Zeiss USA for use of their structured illumination microscopy system. Work in the laboratory of G.W.D. was supported by NIH grants NS059867 and NS039313. T.W. was supported by NIH NRSA postdoc fellowship NIH NINDS 1F32NS081884-01.

References

- Ackley BD, Crew JR, Elamaa H, Pihlajaniemi T, Kuo CJ, Kramer JM. The NC1/endostatin domain of *Caenorhabditis elegans* type XVIII collagen affects cell migration and axon guidance. *J Cell Biol.* 2001; 152:1219–1232. [PubMed: 11257122]
- Ackley BD, Kang SH, Crew JR, Suh C, Jin Y, Kramer JM. The basement membrane components nidogen and type XVIII collagen regulate organization of neuromuscular junctions in *Caenorhabditis elegans*. *J Neurosci.* 2003; 23:3577–3587. [PubMed: 12736328]
- Burrone J, O'Byrne M, Murthy VN. Multiple forms of synaptic plasticity triggered by selective suppression of activity in individual neurons. *Nature.* 2002; 420:414–418. [PubMed: 12459783]
- Chalfie M. Neurosensory mechanotransduction. *Nat Rev Mol Cell Biol.* 2009; 10:44–52. [PubMed: 19197331]
- Chang JH, Javier JA, Chang GY, Oliveira HB, Azar DT. Functional characterization of neostatins, the MMP-derived, enzymatic cleavage products of type XVIII collagen. *FEBS Lett.* 2005; 579:3601–3606. [PubMed: 15978592]
- Cull-Candy SG, Miledi R, Trautmann A, Uchitel OD. On the release of transmitter at normal, myasthenia gravis and myasthenic syndrome affected human end-plates. *J Physiol.* 1980; 299:621–638. [PubMed: 6103954]
- Davis GW. Homeostatic signaling and the stabilization of neural function. *Neuron.* 2013; 80:718–728. [PubMed: 24183022]
- Dhanabal M, Ramchandran R, Waterman MJ, Lu H, Knebelmann B, Segal M, Sukhatme VP. Endostatin induces endothelial cell apoptosis. *J Biol Chem.* 1999; 274:11721–11726. [PubMed: 10206987]
- Dickman DK, Davis GW. The schizophrenia susceptibility gene dysbindin controls synaptic homeostasis. *Science.* 2009; 326:1127–1130. [PubMed: 19965435]
- Felbor U, Dreier L, Bryant RA, Ploegh HL, Olsen BR, Mothes W. Secreted cathepsin L generates endostatin from collagen XVIII. *EMBO J.* 2000; 19:1187–1194. [PubMed: 10716919]
- Frank CA, Kennedy MJ, Goold CP, Marek KW, Davis GW. Mechanisms underlying the rapid induction and sustained expression of synaptic homeostasis. *Neuron.* 2006; 52:663–677. [PubMed: 17114050]
- Goold CP, Davis GW. The BMP ligand Gbb gates the expression of synaptic homeostasis independent of synaptic growth control. *Neuron.* 2007; 56:109–123. [PubMed: 17920019]
- Gottmann K. Transsynaptic modulation of the synaptic vesicle cycle by cell-adhesion molecules. *J Neurosci Res.* 2008; 86:223–232. [PubMed: 17787017]
- Hanai J, Gloy J, Karumanchi SA, Kale S, Tang J, Hu G, Chan B, Ramchandran R, Jha V, Sukhatme VP, et al. Endostatin is a potential inhibitor of Wnt signaling. *J Cell Biol.* 2002; 158:529–539. [PubMed: 12147676]
- Harrington AW, Ginty DD. Long-distance retrograde neurotrophic factor signalling in neurons. *Nat Rev Neurosci.* 2013; 14:177–187. [PubMed: 23422909]
- Heljasvaara R, Nyberg P, Luostarinen J, Parikka M, Heikkila P, Rehn M, Sorsa T, Salo T, Pihlajaniemi T. Generation of biologically active endostatin fragments from human collagen XVIII by distinct matrix metalloproteases. *Exp Cell Res.* 2005; 307:292–304. [PubMed: 15950618]
- Iremonger KJ, Wamsteeker Cusulin JI, Bains JS. Changing the tune: plasticity and adaptation of retrograde signals. *Trends Neurosci.* 2013
- Jakowich SK, Nasser HB, Strong MJ, McCartney AJ, Perez AS, Rakesh N, Carruthers CJ, Sutton MA. Local presynaptic activity gates homeostatic changes in presynaptic function driven by dendritic BDNF synthesis. *Neuron.* 2010; 68:1143–1158. [PubMed: 21172615]
- Kawasaki F, Zou B, Xu X, Ordway RW. Active zone localization of presynaptic calcium channels encoded by the cacophony locus of *Drosophila*. *J Neurosci.* 2004; 24:282–285. [PubMed: 14715960]
- Kim SH, Ryan TA. CDK5 serves as a major control point in neurotransmitter release. *Neuron.* 2010; 67:797–809. [PubMed: 20826311]

- Kim YM, Hwang S, Pyun BJ, Kim TY, Lee ST, Gho YS, Kwon YG. Endostatin blocks vascular endothelial growth factor-mediated signaling via direct interaction with KDR/Flk-1. *J Biol Chem*. 2002; 277:27872–27879. [PubMed: 12029087]
- Kittel RJ, Wichmann C, Rasse TM, Fouquet W, Schmidt M, Schmid A, Wagh DA, Pawlu C, Kellner RR, Willig KI, et al. Bruchpilot promotes active zone assembly, Ca²⁺ channel clustering, and vesicle release. *Science*. 2006; 312:1051–1054. [PubMed: 16614170]
- Liu G, Tsien RW. Properties of synaptic transmission at single hippocampal synaptic boutons. *Nature*. 1995; 375:404–408. [PubMed: 7760934]
- Liu J, Schrank B, Waterston RH. Interaction between a putative mechanosensory membrane channel and a collagen. *Science*. 1996; 273:361–364. [PubMed: 8662524]
- Liu KS, Siebert M, Mertel S, Knoche E, Wegener S, Wichmann C, Matkovic T, Muhammad K, Depner H, Mettke C, et al. RIM-binding protein, a central part of the active zone, is essential for neurotransmitter release. *Science*. 2011; 334:1565–1569. [PubMed: 22174254]
- McCabe BD, Marques G, Haghighi AP, Fetter RD, Crotty ML, Haerry TE, Goodman CS, O'Connor MB. The BMP homolog Gbb provides a retrograde signal that regulates synaptic growth at the *Drosophila* neuromuscular junction. *Neuron*. 2003; 39:241–254. [PubMed: 12873382]
- Meyer F, Moussian B. *Drosophila* multiplexin (Dmp) modulates motor axon pathfinding accuracy. *Dev Growth Differ*. 2009; 51:483–498. [PubMed: 19469789]
- Momota R, Naito I, Ninomiya Y, Ohtsuka A. *Drosophila* type XV/XVIII collagen, Mp, is involved in Wingless distribution. *Matrix Biol*. 2011; 30:258–266. [PubMed: 21477650]
- Muller M, Davis GW. Transsynaptic control of presynaptic Ca²⁺ influx achieves homeostatic potentiation of neurotransmitter release. *Curr Biol*. 2012; 22:1102–1108. [PubMed: 22633807]
- Muller M, Pym EC, Tong A, Davis GW. Rab3-GAP controls the progression of synaptic homeostasis at a late stage of vesicle release. *Neuron*. 2011; 69:749–762. [PubMed: 21338884]
- Myllyharju J, Kivirikko KI. Collagens, modifying enzymes and their mutations in humans, flies and worms. *Trends Genet*. 2004; 20:33–43. [PubMed: 14698617]
- O'Reilly MS, Boehm T, Shing Y, Fukai N, Vasios G, Lane WS, Flynn E, Birkhead JR, Olsen BR, Folkman J. Endostatin: an endogenous inhibitor of angiogenesis and tumor growth. *Cell*. 1997; 88:277–285. [PubMed: 9008168]
- Passos-Bueno MR, Suzuki OT, Armelin-Correa LM, Sertie AL, Errera FI, Bagatini K, Kok F, Leite KR. Mutations in collagen 18A1 and their relevance to the human phenotype. *An Acad Bras Cienc*. 2006; 78:123–131. [PubMed: 16532212]
- Peixoto RT, Kunz PA, Kwon H, Mabb AM, Sabatini BL, Philpot BD, Ehlers MD. Transsynaptic signaling by activity-dependent cleavage of neuroligin-1. *Neuron*. 2012; 76:396–409. [PubMed: 23083741]
- Petersen SA, Fetter RD, Noordermeer JN, Goodman CS, DiAntonio A. Genetic analysis of glutamate receptors in *Drosophila* reveals a retrograde signal regulating presynaptic transmitter release. *Neuron*. 1997; 19:1237–1248. [PubMed: 9427247]
- Pielage J, Cheng L, Fetter RD, Carlton PM, Sedat JW, Davis GW. A presynaptic giant ankyrin stabilizes the NMJ through regulation of presynaptic microtubules and transsynaptic cell adhesion. *Neuron*. 2008; 58:195–209. [PubMed: 18439405]
- Plomp JJ, van Kempen GT, Molenaar PC. Adaptation of quantal content to decreased postsynaptic sensitivity at single endplates in alpha-bungarotoxin-treated rats. *J Physiol*. 1992; 458:487–499. [PubMed: 1302275]
- Seppinen L, Pihlajaniemi T. The multiple functions of collagen XVIII in development and disease. *Matrix Biol*. 2011; 30:83–92. [PubMed: 21163348]
- Sertie AL, Sossi V, Camargo AA, Zatz M, Brahe C, Passos-Bueno MR. Collagen XVIII, containing an endogenous inhibitor of angiogenesis and tumor growth, plays a critical role in the maintenance of retinal structure and in neural tube closure (Knobloch syndrome). *Hum Mol Genet*. 2000; 9:2051–2058. [PubMed: 10942434]
- Suzuki OT, Sertie AL, Der Kaloustian VM, Kok F, Carpenter M, Murray J, Czeizel AE, Kliemann SE, Rosemberg S, Monteiro M, et al. Molecular analysis of collagen XVIII reveals novel mutations, presence of a third isoform, and possible genetic heterogeneity in Knobloch syndrome. *Am J Hum Genet*. 2002; 71:1320–1329. [PubMed: 12415512]

- Wickstrom SA, Alitalo K, Keski-Oja J. Endostatin associates with integrin $\alpha 5 \beta 1$ and caveolin-1, and activates Src via a tyrosyl phosphatase-dependent pathway in human endothelial cells. *Cancer Res.* 2002; 62:5580–5589. [PubMed: 12359771]
- Yamaguchi N, Anand-Apte B, Lee M, Sasaki T, Fukai N, Shapiro R, Que I, Lowik C, Timpl R, Olsen BR. Endostatin inhibits VEGF-induced endothelial cell migration and tumor growth independently of zinc binding. *EMBO J.* 1999; 18:4414–4423. [PubMed: 10449407]
- Younger MA, Muller M, Tong A, Pym EC, Davis GW. A Presynaptic ENaC Channel Drives Homeostatic Plasticity. *Neuron.* 2013
- Zhao C, Dreosti E, Lagnado L. Homeostatic synaptic plasticity through changes in presynaptic calcium influx. *J Neurosci.* 2011; 31:7492–7496. [PubMed: 21593333]

Highlights

1. Multiplexin is a matrix molecule required for presynaptic homeostasis
2. Multiplexin specifies presynaptic calcium channel number and release probability
3. The Endostatin domain of Multiplexin is specific for presynaptic homeostasis
4. Endostatin controls the homeostatic modulation of presynaptic calcium influx

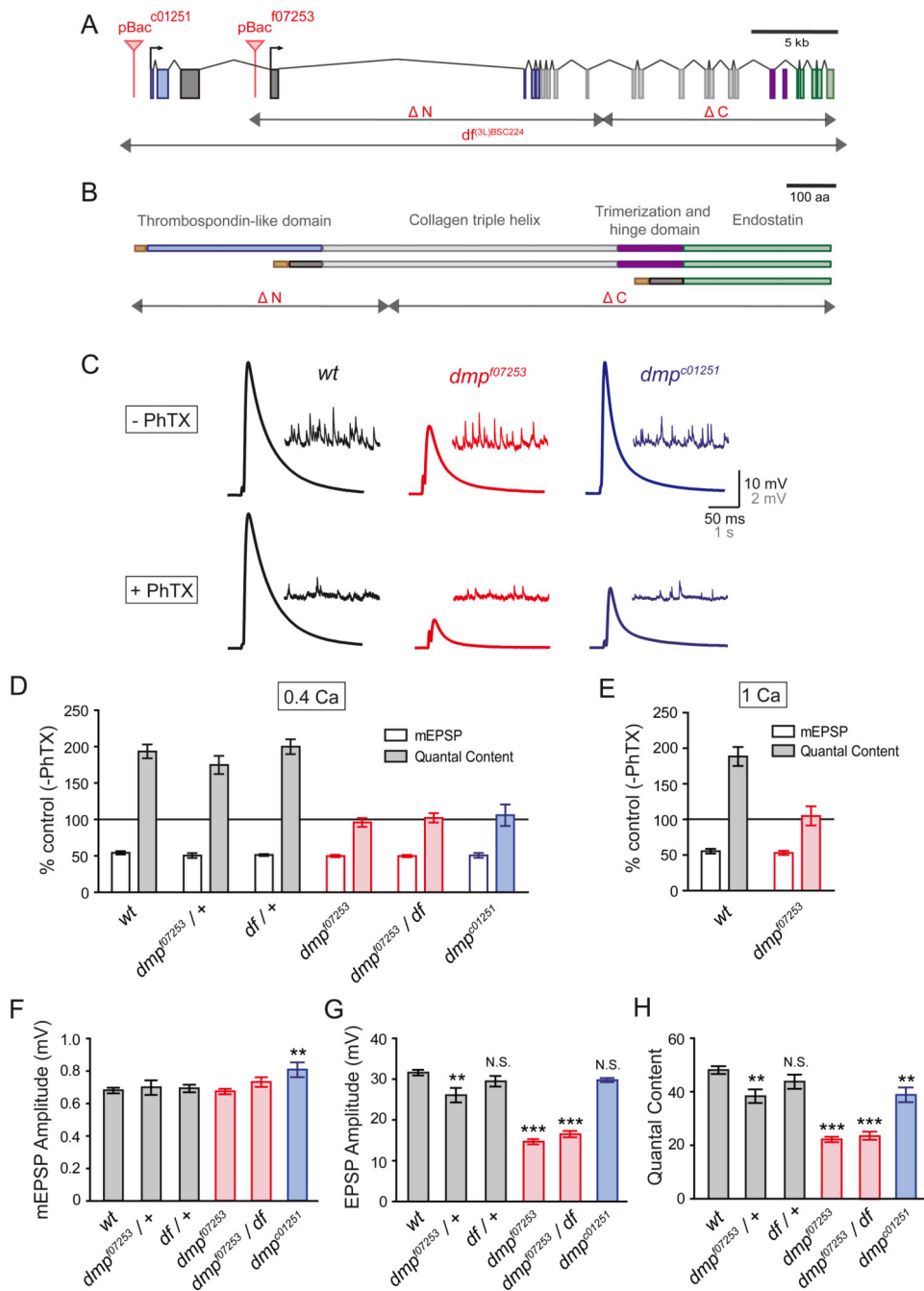


Figure 1. Mutations in *multiplexin* Block Presynaptic Homeostasis

(A) The *Drosophila multiplexin* gene locus. Exons are shown in filled color boxes indicating translated protein domains: blue, Thrombospondin-like domain; dark gray, alternative cap; gray, collagen triple helix domain; purple, trimerization and hinge domain; green, Endostatin domain. Transposon insertions *pBac c01251* and *pBac f07253* reside in introns (red triangles). Genomic deletions at the N-terminal exon 4-11 (ΔN), C-terminal exon 12-25 (ΔC) and deficiency *df^{3L}BSC224* are indicated by gray arrows in the diagram.

(B) Multiplexin protein diagram. Three major protein isoforms are presented. Signal peptides are in brown, and other translated protein domains are presented as in (A). Deletions at the N-terminal exon 4-11 (N) and C-terminal exon 12-25 (C) are indicated by gray arrows in the diagram.

(C) Representative EPSP traces (scale: 10mV, 50ms) and spontaneous mEPSP traces (scale: 2mV, 1s) in the absence and presence of philanthotoxin (-PhTX, +PhTX; top and bottom, respectively) in wild-type (wt, black) and two *multiplexin* mutants (*dmp*^{f07253}, red; *dmp*^{c01251}, blue).

(D) mEPSP amplitudes (open bars) and presynaptic release (quantal content, filled bars) in the presence of PhTX. Average mEPSP amplitude and quantal content are normalized to values in the absence of PhTX for each genotype. The following genotypes are presented: wild-type (wt, gray bars), heterozygous *dmp*^{f07253} mutant (*dmp*^{f07253/+}, gray bars), heterozygous *df*^{(3L)BSC224} mutant (*df*⁺, gray bars), homozygous *dmp*^{f07253} mutant (*dmp*^{f07253}, red bars), *dmp*^{f07253} placed *in trans* to a deficiency *df*^{(3L)BSC224} (*dmp*^{f07253/df}, red bars), and homozygous *dmp*^{c01251} mutant synapses (*dmp*^{c01251}, blue bars).

(E) mEPSP amplitude (open bars) and presynaptic release (quantal content, filled bars) in the presence of PhTX recorded at 1mM calcium. Average mEPSP amplitude and quantal content are normalized to values in the absence of PhTX. Wild-type (wt, gray bars) and homozygous *dmp*^{f07253} mutant synapses (*dmp*^{f07253}, red bars) are presented.

(F) - (H) Baseline transmission for *multiplexin* mutants. Average mEPSP amplitude (F), EPSP amplitude (G) and presynaptic release (quantal content, H) in the absence of PhTX. Genotypes are presented the same as in (D). Mean \pm SEM; **p < 0.005, ***p < 0.001, N.S. not significant; Student's t-test.

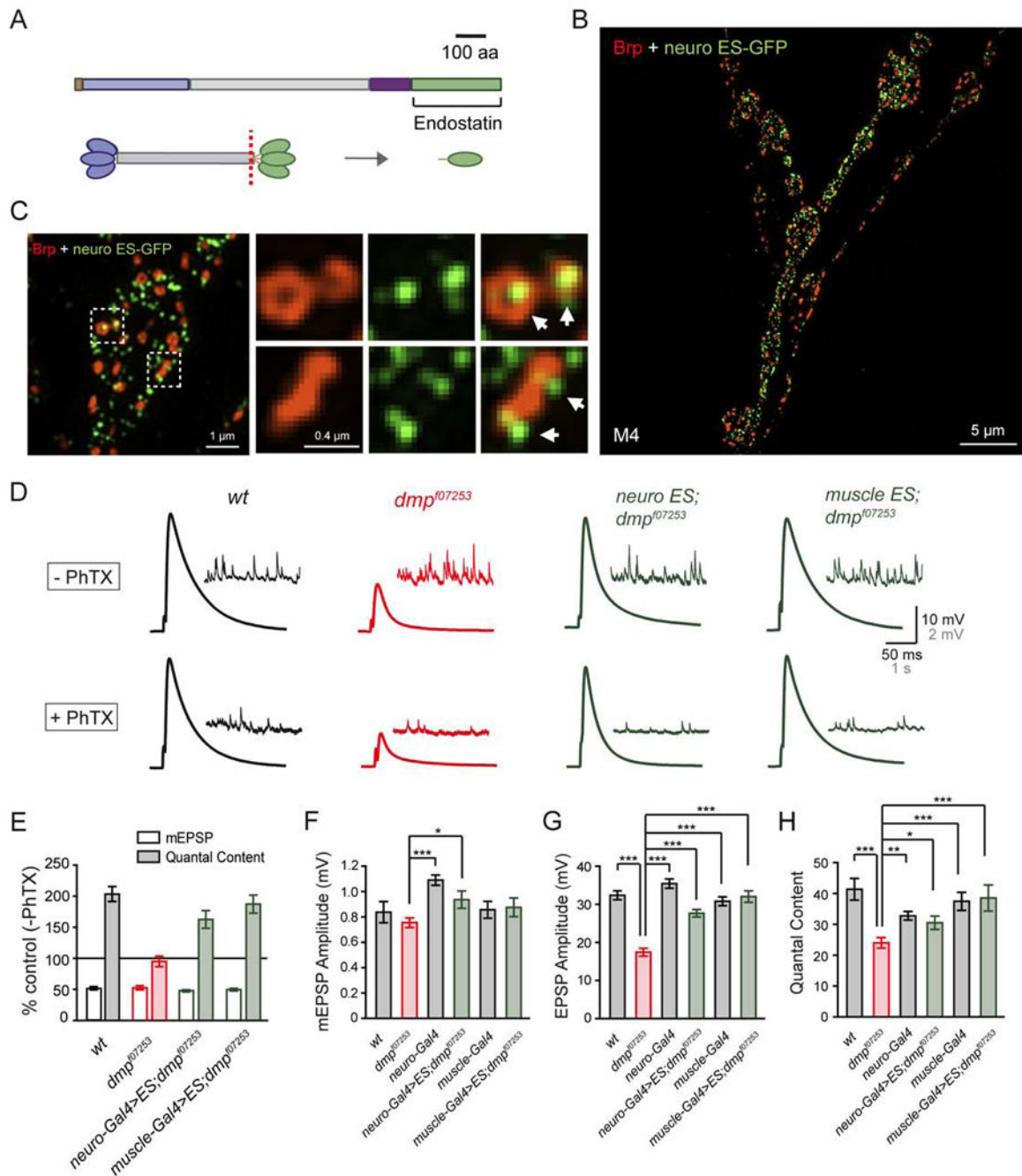


Figure 2. Transgenic Endostatin Restores Baseline Neurotransmission and Synaptic Homeostasis when Expressed either Pre- or Postsynaptically

(A) A diagram for the generation of Endostatin. Translated protein domains of Multiplexin (upper panel) are indicated by filled boxes as in Figure 1B. C-terminal domain of Multiplexin can be cleaved proteolytically (red dotted line, lower panel) at hinge region to release monomers of Endostatin (green oval).

(B) A representative Structured Illumination Microscopy (SIM) image of overexpressed Endostatin-GFP. Neuronal-specific expression of Endostatin-GFP (*elav^{C155}-Gal4>UAS-*

endostatin-GFP, neuro ES-GFP, green) and immuno-labeled Bruchpilot (Brp, red) on muscle 4 (M4) are shown at low magnification.

(C) Representative SIM images of neuronal specific expression of Endostatin-GFP (neuro ES-GFP, green) and immuno-labeled Bruchpilot (Brp, red) are shown at higher magnification. Note the relative localization of Endostatin to ring-shaped active zones (white arrows, right panels).

(D) Representative EPSP (scale: 10mV, 50ms) and spontaneous mEPSP (scale: 2mV, 1s) traces in the absence and presence of PhTX (-PhTX, +PhTX; top and bottom, respectively) in wild-type (wt, black), homozygous *multiplexin dmp^{f07253}* mutant (*dmp^{f07253}*, red) and *dmp^{f07253}* mutant synapses bearing an Endostatin overexpression construct (*UAS-endostatin*) driven by *elav^{C155}-Gal4* (*neuro ES;dmp^{f07253}*, green) or by *MHC-Gal4* (*muscle ES;dmp^{f07253}*, green, right panel).

(E) mEPSP amplitude (open bars) and presynaptic release (quantal content, filled bars) in the presence of PhTX. Average mEPSP amplitude and quantal content are normalized to values in the absence of PhTX for each genotype. The following genotypes are presented: wild-type (wt, gray bars), *multiplexin dmp^{f07253}* mutant (*dmp^{f07253}*, red bars) and presynaptically (*neuro ES;dmp^{f07253}*, green bars), or postsynaptically (*muscle ES;dmp^{f07253}*, green bars) expressed Endostatin in the *dmp^{f07253}* mutant background.

(F) - (H) Average mEPSP amplitude (F), EPSP amplitude (G) and presynaptic release (quantal content, H) in the absence of PhTX. The following genotypes are presented: wild-type (wt, gray bars), *multiplexin dmp^{f07253}* mutant (*dmp^{f07253}*, red bars), neural specific Gal4 driver (neuro-Gal4, gray bars), presynaptically expressed Endostatin in *dmp^{f07253}* mutant background (*neuro ES;dmp^{f07253}*, green bars), muscle specific Gal4 driver (muscle-Gal4, gray bars) and postsynaptically expressed Endostatin in the *dmp^{f07253}* mutant background (*muscle ES;dmp^{f07253}*, green bars). Mean \pm SEM; *p < 0.05, ***p < 0.001; Student's t-test.

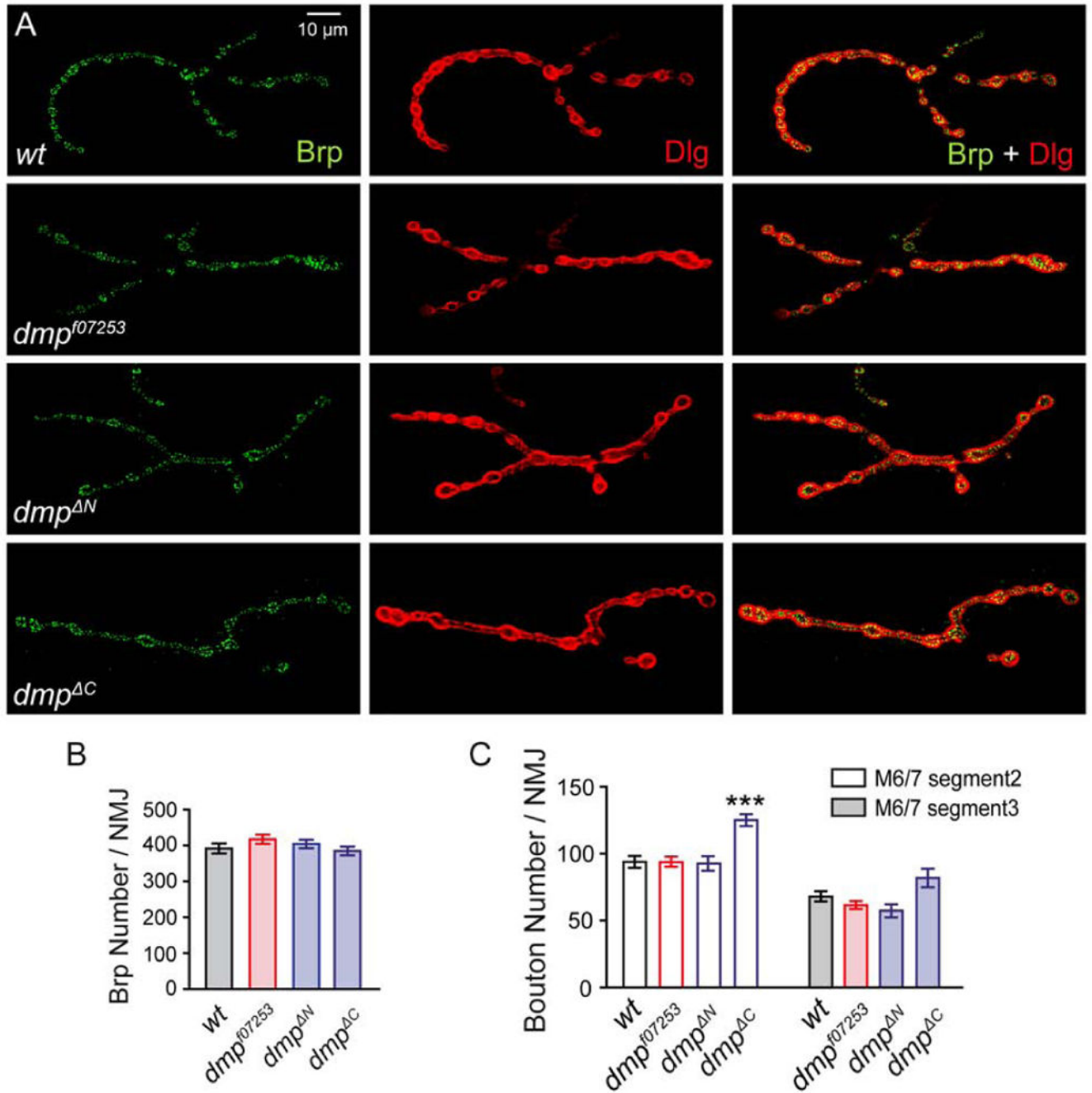


Figure 3. Multiplexin Mutants Have Normal Synaptic Morphology

(A) Representative images of the NMJ in wild-type (wt), the *multiplexin dmp^{f07253}* mutant (*dmp^{f07253}*), as well as the N- and C-terminal deletion mutants (*dmp^N* and *dmp^C*) on muscle 4 (M4). NMJ are immuno-labeled with presynaptic Bruchpilot (Brp, green) and postsynaptic discs large (Dlg, red).

(B) The average number of presynaptic Brp puncta per NMJ at muscle 4 is unaltered in *multiplexin* mutants. The following genotypes are presented: wild-type (wt, n=26 NMJ, gray bar), *multiplexin dmp^{f07253}* mutant (*dmp^{f07253}*, n=19, red bar), *multiplexin* N-terminal

deletion mutant (*dmp*^N, n=20, blue bar), and C-terminal deletion mutant NMJ (*dmp*^C, n=18, blue bar).

(C) Average number of boutons on muscle 6/7 in abdominal segment 2 (open bars) and 3 (filled bars) are normal in *multiplexin* mutants. Wild-type (wt, n=19 NMJ, gray bars), *multiplexin dmp*^{f07253} mutant (*dmp*^{f07253}, n=19, red bars), *multiplexin* N-terminal deletion mutant (*dmp*^N, n=7, blue bars), and C-terminal deletion mutant synapses (*dmp*^C, n=8, blue bars) are presented.

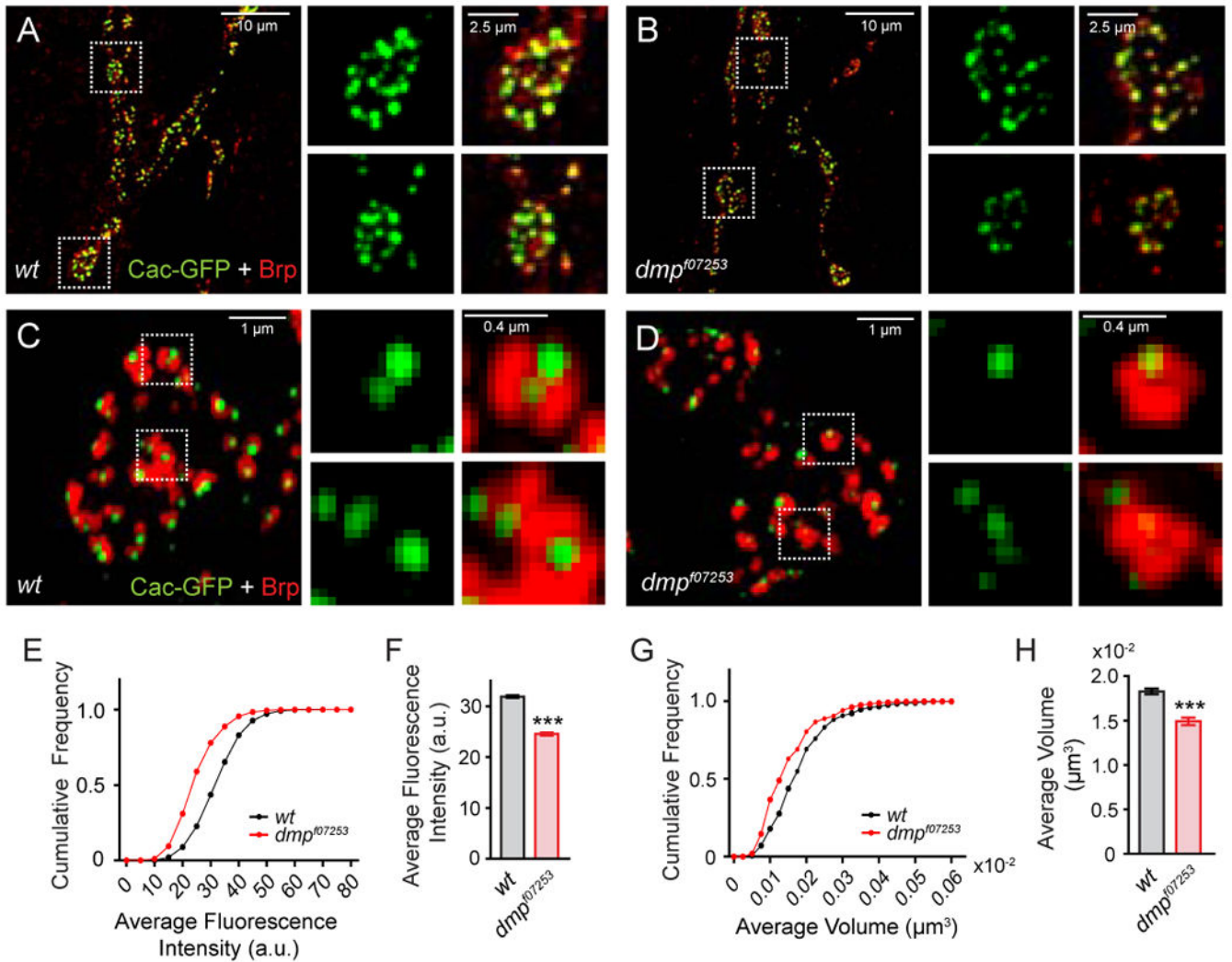


Figure 4. Decreased Calcium Channel Abundance at the *multiplexin* NMJ

(A) - (B) Representative confocal microscopy images of presynaptically expressed GFP-tagged calcium channel subunit (*elav^{C155}-Gal4>UAS-Cac-GFP*, green) in wild-type (A, wt) and *multiplexin* mutant (B, *dmp^{f07253}*) NMJ at muscle 6/7. NMJs are co-labeled with presynaptic Bruchpilot (Brp, red). Representative boutons (white boxes) are shown in higher magnification in right panels.

(C)- (D) Representative structured illumination microscopy (SIM) images of Cac-GFP (green) and Brp (red) in wild-type (C, wt) and *multiplexin* mutant (D, *dmp^{f07253}*) NMJ on muscle 6/7 (M6/7). Representative ring-shaped active zones and Cac-GFP puncta (white boxes, left panels) are presented in higher magnification in right panels.

(E)- (F) Quantification of average Cac-GFP fluorescence intensity (a.u., arbitrary unit) within Brp puncta. Cumulative frequencies (E) and mean values (F) of average Cac-GFP intensities within Brp puncta on muscle 6/7 in wild-type (wt, n=1463 puncta, 7 NMJ, gray line and bars) and *multiplexin* mutant NMJ (*dmp^{f07253}*, n=875 puncta, 7NMJ, red line and bars).

(G) - (H) Quantification of average volumes for Cac-GFP puncta that associate with Brp. Cumulative frequencies (G) and mean values (H) of average Cac-GFP volume on muscle 6/7 (M6/7) in wild-type (wt, n=914 puncta, 7 NMJ, gray line and bars) and *multiplexin* mutant NMJ (*dmp*^{f07253}, n=918 puncta, 5 NMJ, red line and bars). Mean \pm SEM; ***p < 0.001; Student's t-test.

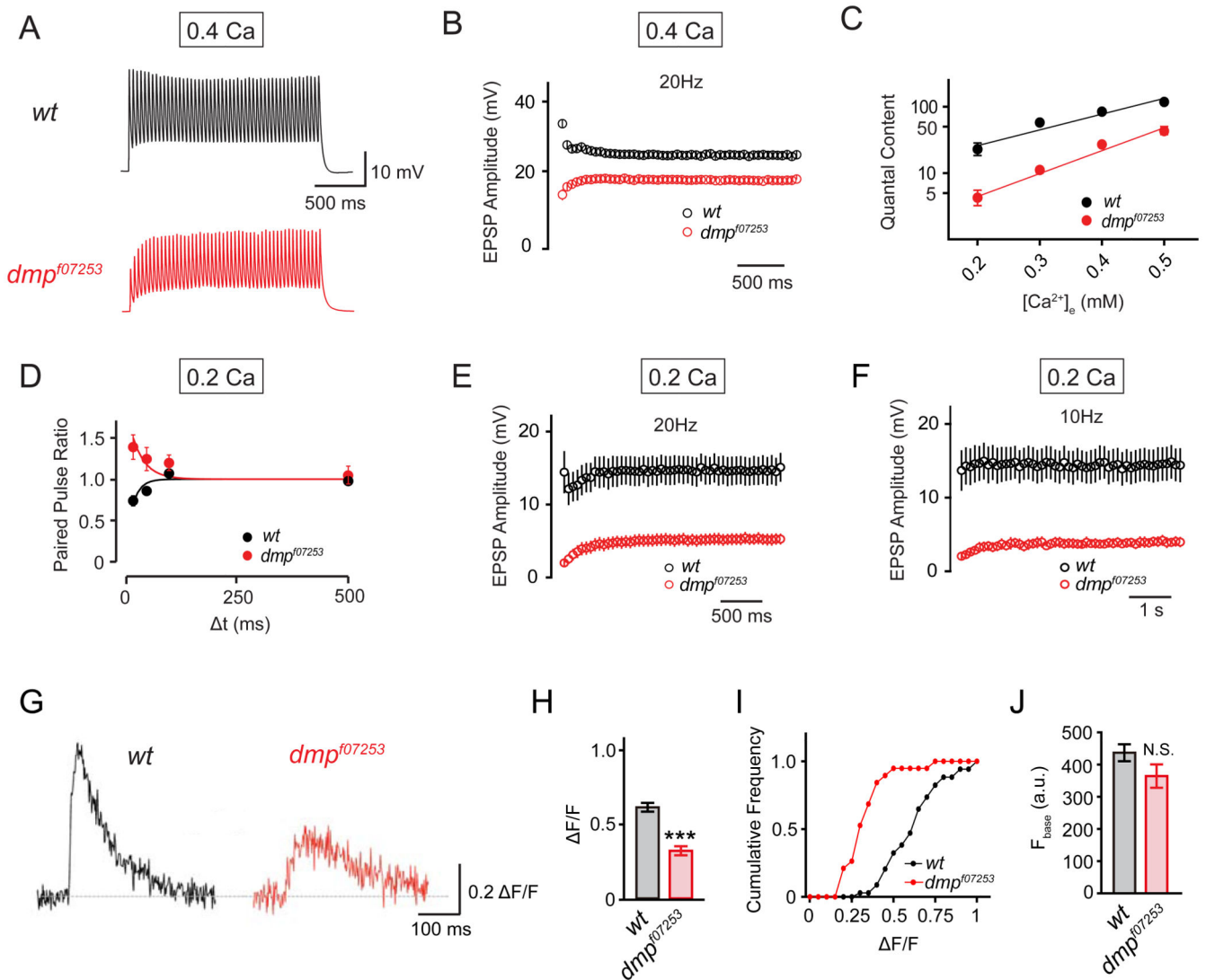


Figure 5. Decreased Presynaptic Calcium Influx and Release Probability at the *multiplexin* NMJ
 (A) Representative EPSP trains (scale: 10mV, 500ms) for wild-type (wt, black), *dmp^{f07253}* mutant (*dmp^{f07253}*, red) NMJ in response to 20Hz (50 stimuli) stimulation in 0.4mM extracellular calcium.

(B) Average EPSP amplitudes during 20Hz (50 stimuli) stimulation for wild-type (wt, n=11, black) and *dmp^{f07253}* mutant NMJ (*dmp^{f07253}*, n=9, red).

(C) Quantification of single action potential (AP)-evoked quantal content for wild-type (wt, black) and *dmp^{f07253}* mutant NMJ (*dmp^{f07253}*, red) at different extracellular calcium concentrations. Wild-type, n=8, 5, 18, 7; *dmp^{f07253}*, n=9, 12, 31, 11 for calcium concentrations of 0.2, 0.3, 0.4, 0.5mM respectively. Quantal content values are corrected for non-linear summation throughout.

(D) Paired-pulse ratio (the ratio between the amplitudes of the second and first EPSPs) at different inter-stimulus intervals for wild-type (wt, n=9, black) and *dmp^{f07253}* mutant NMJ (*dmp^{f07253}*, n=10, red) in 0.2mM extracellular calcium. Wild-type and *multiplexin* mutant data are fit with exponential increase and decay functions.

(E) - (F) Average EPSP amplitudes during 20Hz (E, 50 stimuli) and 10Hz (F, 50 stimuli) train stimulation for wild-type (wt, 20Hz, n=9; 10Hz, n=9, black), and *dmp^{f07253}* mutant NMJ (*dmp^{f07253}*, 20Hz, n=12; 10Hz, n=12, red) in 0.2mM extracellular calcium.

(G) Representative traces of single AP-evoked, spatially averaged calcium transients measured by line scans of a wild-type (wt, left) and a *dmp^{f07253}* mutant NMJ (*dmp^{f07253}*, right).

(H) - (I) Average calcium transient peak amplitudes (H, $\Delta F/F$) and cumulative frequencies of $\Delta F/F$ peak amplitudes (I) for wild-type (wt mean = 0.62 ± 0.033 SEM, n=34 boutons, gray bar and line) and *dmp^{f07253}* mutant boutons (*dmp^{f07253}* mean = 0.32 ± 0.31 , n=19 boutons, red bar and line).

(J) Average baseline fluorescence (F_{base}) for wild-type (wt, gray bar) and mutant boutons (*dmp^{f07253}*, red bar). Mean \pm SEM; ***p < 0.001, N.S. not significant; Student's t-test.

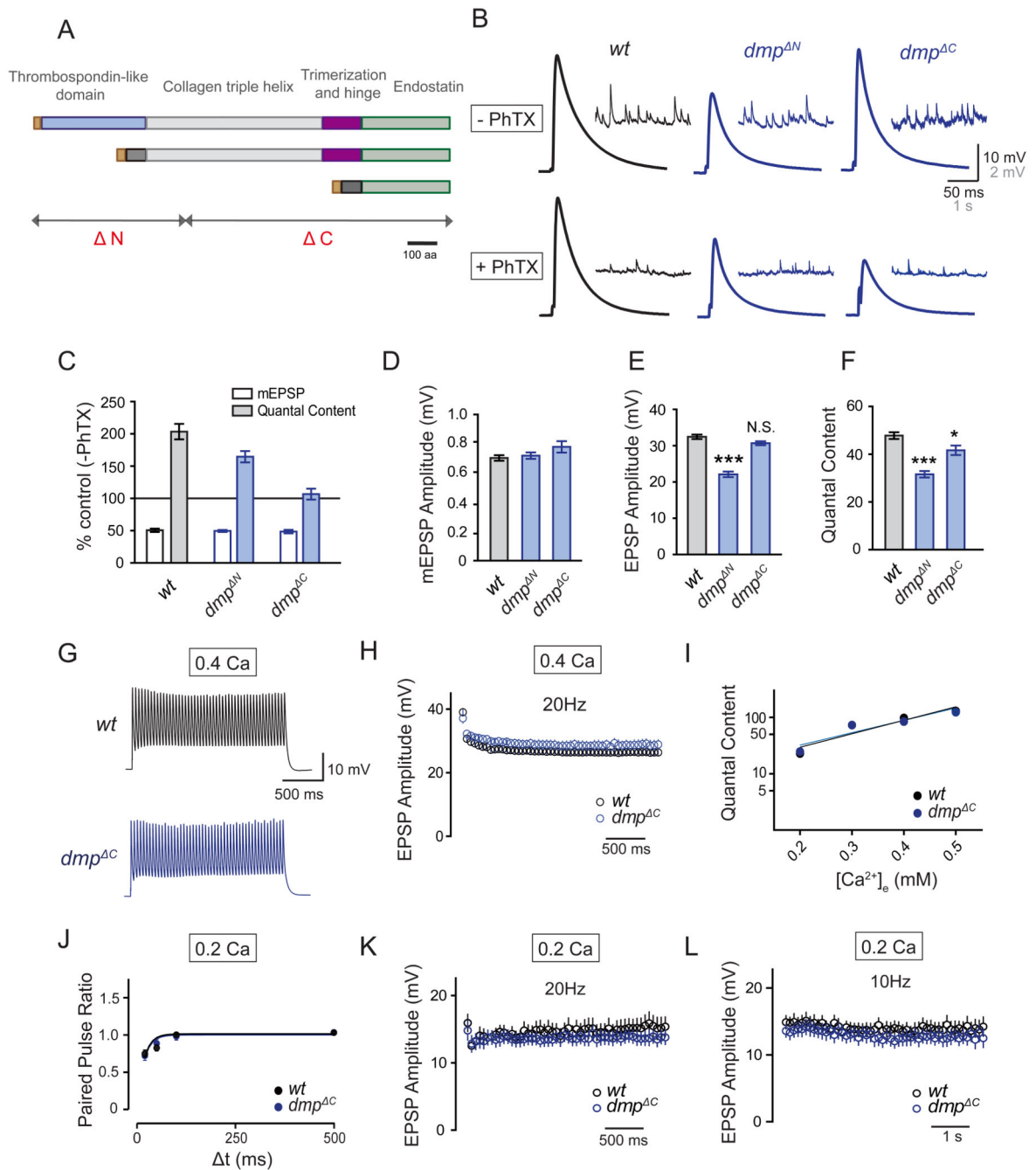


Figure 6. Different Activities are Contributed by the N- and C-terminal Domains of Multiplexin
(A) Multiplexin protein diagram. Three major protein isoforms are presented. Deletions at the N-terminal (ΔN), C-terminal (ΔC) domains are indicated by gray arrows in the diagram.
(B) Representative EPSP (scale: 10mV, 50ms) and spontaneous mEPSP (scale: 2mV, 1s) traces in the absence and presence of PhTX (-PhTX, +PhTX; top and bottom respectively) in wild-type (wt, black), *multiplexin* N-terminal (*dmp^{ΔN}*, blue, middle panel), and C-terminal (*dmp^{ΔC}*, blue, right panel) deletion mutations.

(C) The Multiplexin C-terminal Endostatin domain is necessary for a homeostatic compensatory increase in transmitter release. mEPSP amplitudes (open bars) and presynaptic release (quantal content, filled bars) in the presence of PhTX. Average mEPSP amplitudes and quantal content are normalized to values in the absence of PhTX for each genotype. The following genotypes are presented: wild-type (wt, gray bars), *multiplexin* N-terminal deletion mutant (*dmp^N*, blue bars), C-terminal deletion mutant synapses (*dmp^C*, blue bars).

(D) - (F) The *multiplexin* N-terminal deletion mutant has a basal neurotransmission defect. Average mEPSP amplitude (D), EPSP amplitude (E) and presynaptic release (quantal content, F) in the absence of PhTX. Genotypes are presented the same as in (B). Mean \pm SEM; * $p < 0.05$, *** $p < 0.001$, N.S. not significant; Student's t-test.

(G) Representative EPSP trains (scale: 10mV, 500ms) for wild-type (wt, black), and *dmp^C* (blue) synapses in response to 20Hz (50 stimuli) stimulation at 0.4mM extracellular calcium.

(H) Average EPSP amplitude during 20Hz (50 stimuli) train for wild-type (wt, n=12, black), and *dmp^C* mutant synapses (*dmp^C*, n=7, blue).

(I) Calcium cooperativity of transmitter release at wild-type and *dmp^C* mutant synapses. Quantification of single action potential (AP)-evoked EPSP quantal contents for wild-type (wt, black) and *dmp^C* mutant (*dmp^C*, blue) at different extracellular calcium concentrations. Wild-type, n=14, 8, 16, 8; *dmp^C*, n=17, 8, 8, 7 for calcium concentration 0.2, 0.3, 0.4, 0.5mM respectively.

(J) Paired-pulse ratio at different inter-stimulus intervals for wild-type (wt, n=9, black) and *dmp^C* mutant (*dmp^C*, n=9, blue) at 0.2mM extracellular calcium. Wild-type and *dmp^C* mutant data are fit with exponential increase function.

(K) - (L) Average EPSP amplitude during 20Hz (K, 50 stimuli) and 10Hz (L, 50 stimuli) train for wild-type (wt, 20Hz, n=11; 10Hz, n=9, black), and *dmp^C* mutant synapses (*dmp^C*, 20Hz, n=11; 10Hz, n=10, blue).

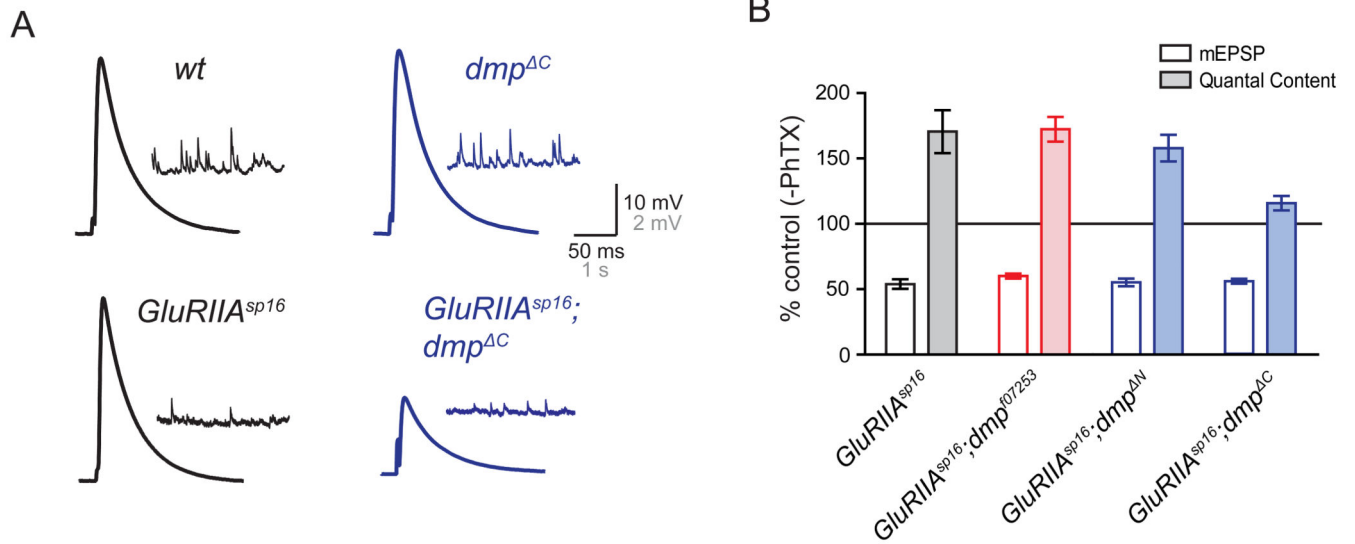


Figure 7. Endostatin is Required for the Long-term Maintenance of Presynaptic Homeostasis

(A) Representative EPSP (scale: 10mV, 50ms) and mEPSP (scale: 2mV, 1s) traces in wild-type (A, *wt*, black), *multiplexin* C-terminal deletion mutant (B, *dmp^{ΔC}*, blue), *GluRIIA^{sp16}* (C, *GluRIIA^{sp16}*, black), and *GluRIIA^{sp16}; dmp^{ΔC}* double mutant NMJ (D, *GluRIIA^{sp16}; dmp^{ΔC}*, blue).

(B) Quantification of mEPSP amplitude (open bars) and presynaptic release (quantal content, filled bars). Average mEPSP amplitudes and quantal content are normalized to baseline values for wild-type and *multiplexin* mutants. The following genotypes are presented: *GluRIIA^{sp16}* (gray bars), *GluRIIA^{sp16}; dmp^{f07253}* (red bars), *GluRIIA^{sp16}; dmp^{ΔN}* (blue bars), and *GluRIIA^{sp16}; dmp^{ΔC}* mutant (blue bars).

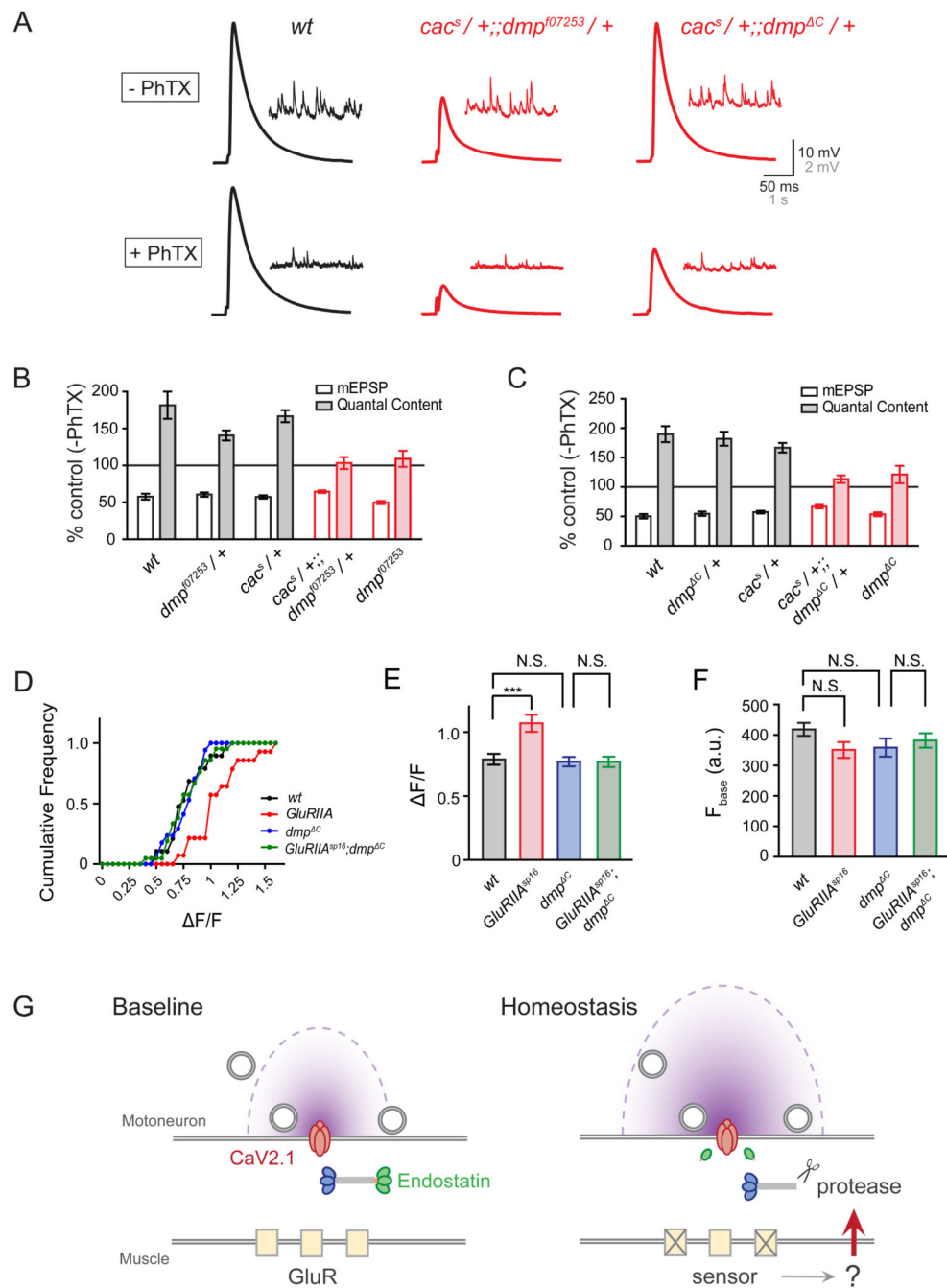


Figure 8. Multiplexin Genetically Interacts with the Pore-Forming α Subunit of the CaV2.1 Calcium Channel and Controls Homeostatic Increase in Presynaptic Calcium Influx

(A) Representative EPSP (scale: 10mV, 50ms) and spontaneous mEPSP (scale: 2mV, 1s) traces in the absence and presence of PhTX (-PhTX, +PhTX; top and bottom respectively) in wild-type (wt, black) and heterozygous *cac^s* mutant placed *in trans* with *dmp^{f07253}* (*cac^s/+;;dmp^{f07253}/+*, red) and *dmp^C* (*cac^s/+;;dmp^C/+*, red) mutants.

(B) A homeostatic increase in quantal content following PhTX treatment is blocked when heterozygous mutants of *dmp^{f07253}* and *cac^s* are placed *in trans*. mEPSP amplitude (open

bars) and presynaptic release (quantal content, filled bars) in the presence of PhTX. The following genotypes are presented: wild-type (wt, gray bars), heterozygous *dmp^{f07253}* mutant (*dmp^{f07253}/+*, gray bars), heterozygous *cac^s* mutant (*cac^s/+*, gray bars), heterozygous mutants of *dmp^{f07253}* and *cac^s* placed *in trans* (*cac^s/+; dmp^{f07253}/+*, red bars), and homozygous *dmp^{f07253}* mutant NMJ (*dmp^{f07253}*, red bars).

(C) Synaptic homeostasis is blocked in a trans-heterozygous mutant of *dmp^C* and calcium channel subunit *cac^s*. The following genotypes are presented: wild-type (wt, gray bars), heterozygous *dmp^C* mutant (*dmp^C/+*, gray bars), heterozygous *cac^s* (*cac^s/+*, gray bars), heterozygous mutants of *dmp^C* and *cac^s* placed *in trans* (*cac^s/+; dmp^C/+*, red bars), homozygous *dmp^C* mutant NMJ (*dmp^C*, red bars).

(D) - (E) Cumulative frequencies of F/F peak amplitudes (D) and average calcium transient peak amplitudes (E, F/F) and for wild-type (wt, n= 19 boutons, gray line and bar), *GluRIIA^{sp16}* (*GluRIIA^{sp16}*, n= 14 boutons, red line and bar), *dmp^C* (*dmp^C*, n=17 boutons, blue line and bar) and *GluRIIA^{sp16}; dmp^C* mutant boutons (*GluRIIA^{sp16}; dmp^C*, n=21 boutons, green line and bar).

(F) Average baseline fluorescence (F_{base}) for wild-type (wt, gray line and bar), *GluRIIA^{sp16}* (*GluRIIA^{sp16}*, red line and bar), *dmp^C* (*dmp^C*, blue line and bar) and *GluRIIA^{sp16}; dmp^C* double mutant boutons (*GluRIIA^{sp16}; dmp^C*, green line and bar). Mean \pm SEM; *** $p < 0.001$, N.S. not significant; Student's t-test.

(G) Model for Endostatin dependent regulation of synaptic homeostasis. Multiplexin is required for both baseline transmission and synaptic homeostasis at *Drosophila* NMJ. Under normal conditions (Baseline, left panel), we propose that Multiplexin (trimer diagrammed and labeled as “Endostatin” in green) resides in extracellular matrix at the synaptic cleft where it associates with and stabilizes presynaptic calcium channels (light red channel). This activity is necessary for normal basal synaptic transmission and requires the N-terminal Thrombospondin-like domain of Multiplexin. During presynaptic homeostasis (Homeostasis, right panel), when postsynaptic glutamate receptor function is inhibited pharmacologically or genetically (cross-hatched yellow boxes), Multiplexin is proteolytically cleaved by an as yet unidentified protease that is either resident in the synaptic cleft or secreted postsynaptically (red arrow and scissors). Proteolytic cleavage releases Endostatin (green oval), which is necessary for the homeostatic potentiation of presynaptic calcium influx (purple micro-domain) through the CaV2.1 calcium channel. The potentiation of presynaptic calcium influx provides access to previously inaccessible, but release-ready, synaptic vesicles.